European Journal of Pharmaceutical Sciences 111 (2018) 238–246

Contents lists available at ScienceDirect

European Journal of Pharmaceutical Sciences

journal homepage: www.elsevier.com/locate/ejps

Tuning the rheological properties of an ammonium methacrylate copolymer for the design of adhesives suitable for transdermal patches

Gaia M.G. Quaroni[a], Chiara G.M. Gennari[a], Francesco Cilurzo[a,*], Guylaine Ducouret[b], Costantino Creton[b,c], Paola Minghetti[a]

[a] Department of Pharmaceutical Sciences, Università degli Studi di Milano, via G. Colombo, 71, 20133 Milano, Italy
[b] Laboratory of Soft Matter And Engineering Sciences, CNRS UMR 7615, École SupÉrieure de Physique et de Chimie Industrielles de la Ville de Paris (ESPCI), ParisTech, PSL Research Univeristy, 10 rue Vauquelin, F-75231 Paris cedex 05, France
[c] IMM, UPMC Univ Paris 06, Sorbonne-UniversitÉs, 10 rue Vauquelin, F-75231 Paris cedex 05, France

ARTICLE INFO

Keywords:
Eudragit RL
Pressure-sensitive adhesives
Transdermal patches
Rheology
Skin permeation
Drug release

ABSTRACT

Eudragit® RL (EuRL) matrices have been proposed to release a drug to the skin. However, no information is available on both viscoelastic and adhesive properties of such compositions. This work focuses on the evaluation of both rheological and texture properties of EuRL differently plasticized with tributyl citrate (TBC) or triacetin (TRI) in order to design a pressure sensitive adhesive suitable for transdermal patch preparation. The patch adhesive properties (*i.e.* tack, peel adhesion and shear adhesion) as well as its *in vitro* biopharmaceutical performances were determined after loading ibuprofen, ketoprofen or flurbiprofen. The addition of 40–60% w/w TBC or 40–50% w/w TRI to EuRL permitted to obtain matrices with the desired adhesive properties. Moreover, the increase of plasticizer content and loading of the drug reduced the relaxation time (τ_R). Consequently, the shear adhesion values decreased and the *in vitro* drug release constants (k) increased. Indeed, the k values from patches containing TBC were lower than the corresponding with TRI because of the lower fluidity of such matrices. In conclusion, the 60/40 EuRL/TBC binary blend is suitable for the design of transdermal patches since the *in vitro* permeability of the three selected drugs appeared comparable to those described in literature for marketed products.

1. Introduction

Transdermal patches and medicated plasters are pharmaceutical preparations designed to provide a prolonged delivery of drugs to the skin to achieve a systemic or local effect, respectively. Usually, they are drug-in-adhesive systems, in which the drug is dispersed and/or dissolved in a pressure-sensitive adhesive (PSA) matrix. PSAs are defined as soft polymeric materials that display an instantaneous adhesion on almost any surface by simple contact under a light pressure and that can ideally be detached from the substrate without any residue (Tan and Pfister, 1999).

The efficiency of the therapeutic treatment by these dosage forms is related not only to their ability to release the drug through the skin, but also to their complete skin contact over the whole delivery surface for the entire treatment period. If the patch lifts or partially detaches, the effective contact area, and thus the drug absorption, is unpredictable and therapeutic failure can occur (Fauth et al., 2002).

The adhesion properties of a PSA strongly depend on their viscoelastic properties. Viscoelastic materials are needed in order to relax stresses, easily create a molecular contact, and dissipate energy upon debonding. Indeed, PSAs should be soft and relax stresses to favor the contact with the substrate (Creton and Leibler, 1996), but they should also be highly dissipative and lightly physically or chemically crosslinked to resist to the applied stress once the bond is formed. From a technological point of view, the PSA matrix is characterized by tack, peel adhesion and resistance to shear. Tack is the property that enables an adhesive to form a bond with the surface of another material upon brief contact and under light pressure; peel adhesion is the force required to peel away a patch from a surface; shear adhesion represents the resistance of the matrix to flow over long times and moderate loads (Cilurzo et al., 2012).

The literature reports the feasibility to design PSAs able to deliver several drugs made from a poly(ethylacrylate-*co*-methylmethacrylate-*co*-trimethylammonioethylmethacrylate chloride), traded with the name of Eudragit® RL PO (EuRL) (Cilurzo et al., 2014). However, no information is available about either the viscoelastic behavior or the

* Corresponding author.
E-mail address: francesco.cilurzo@unimi.it (F. Cilurzo).

http://dx.doi.org/10.1016/j.ejps.2017.10.006
Received 14 July 2017; Received in revised form 13 September 2017; Accepted 4 October 2017
Available online 05 October 2017

adhesive properties of such compositions.

This study focuses on the evaluation of the viscoelastic and adhesive properties of PSAs made of EuRL differently plasticized in order to identify a matrix suitable to develop a patch and clarify the possible relationships between the main rheological descriptors and the adhesive properties of such patch and the drug release pattern. This kind of relationship is rarely investigated, although it could provide useful information to design both transdermal patches and medicated plasters in the attempt to optimize their performance.

To achieve this goal, several PSAs were designed by mixing EuRL in different ratios (40–60% w/w) with two plasticizers, namely triacetin (TRI) and tributyl citrate (TBC). The drug release properties of the optimal combinations were evaluated by adding three different drugs, namely ibuprofen, flurbiprofen and ketoprofen. PSAs were characterized in terms of rheological and tack properties. Probe tack tests were performed not only to evaluate the adhesive properties of the PSAs, but mainly to understand better the debonding mechanisms (Deplace et al., 2009; Nase et al., 2008). The patches were characterized by measuring shear and peel adhesion and cold flow, which refers to the dimensional change and/or deformation of the polymeric matrix of a patch beyond the boundaries (EMA, 2014). The drug release pattern was determined by both *in vitro* dissolution test and *in vitro* skin permeation using human epidermis as membrane.

2. Materials and methods

2.1. Materials

Poly(ethylacrylate-*co*-methylmethacrylate-*co*-trimethylammonioethylmethacrylate chloride), traded with the name of Eudragit® RL PO (EuRL), with molar ratio of 1:2:0.2 and molecular weight 32 kDa, was kindly donated by Rofarma Italia (Gaggiano, Italy). Tributyl citrate (Citroflex 4, TBC) was supplied by Morflex (Greensboro, USA) and triacetin (TRI), ethyl acetate (EtOAc) and isopropanol (iPrOH) were purchased from Sigma Aldrich (Milan, Italy). The release liner used for patch preparation was a siliconized polyester film from Saint Gobain kindly donated by Bouty (Cassina de Pecchi, Italy), while the backing layer was a polyester film with a thickness of 57 μm (Polifibra, Agrate Brianza, Italy). Three active ingredients were selected: *S*-ibuprofen (IB) was purchased from Dipharma Francis (Baranzate, Italy); ketoprofen (KP), and flurbiprofen (FP) from Farmalabor (Canosa di Puglia, Italy). All solvents were of analytical grade, unless specified.

2.2. Blend preparation

To obtain the EuRL organic dispersion, the powder was dispersed in the solvent, ethyl acetate or isopropanol, at the concentration of 40% w/w. The polymeric blends were prepared by adding the plasticizer (TBC or TRI) to the EuRL dispersions. The amount of TBC or TRI ranged between 40 and 60% with respect to EuRL weight. When the active ingredient (*i.e.* IB, KP or FP) was added to EuRL mixture, it was preliminarily dissolved in the plasticizer and, then, added to the polymeric dispersion. The drug content was 4% w/w calculated on EuRL weight.

The polymeric dispersion was mixed for 3 h at 60 °C with a magnetic stirrer of 100 rpm. One night of rest was necessary in order to reduce the air bubbles formed during the stirring and to favor the full swelling of the polymeric chains.

2.3. Rheological properties in the linear regime

The rheological characteristics were measured on a Discovery Hybrid Instrument HR-3 (TA Instruments, New Castle, USA). The frequency-dependence of the viscoelastic moduli G′ and G″ was characterized with a parallel plate geometry (diameter 20 mm), by using a crosshatched upper plate for the formulations containing the lower amount of plasticizer, and a sandblasted plate for the other formulations.

2.3.1. Sample preparation

In order to obtain equilibrated samples of about 1 mm thickness, a special sample holder was used. The device consisted of lower plate geometry, to which a ring was fixed through a Teflon tape; this particular device allowed to put 10–15 mL (depending on the plasticizer concentration) of solution and completely dry it (slowly drying in air for 48 h, and then 30 min of drying at 45 °C); the same sample holder was used to test the sample on the rheometer by simply removing the holding ring just before the analysis (after the 7 days required for matrices maturation).

2.3.2. Experimental setup

To evaluate the linear viscoelastic regime, a strain-sweep procedure at 1 Hz was performed; then, a frequency-sweep deformation (0.01–100 rad/s) was applied to the sample, and the resulting response in terms of stress was measured. Each sample was analyzed first at 25 °C, and then at 32 °C. The analyses were performed in triplicate to verify the reproducibility of the experimental conditions.

More details on the significance of this type of experiments are summarized in Appendix B.

2.4. ATR-FTIR spectroscopy

Attenuated total reflectance Fourier transform infrared (ATR-FTIR) spectra were recorded over the wavenumber region 4000–650 cm^{-1} with an ATR-FTIR spectrometer (Perkin Elmer, Waltham, USA), equipped with a diamond crystal. For each sample 256 scans were collected at a resolution of 2 cm^{-1}. Spectra were ATR corrected and smoothed and then analyzed by using Origin Pro (Origin Lab). The maximum absorbance of peaks in the 1650 and 1800 cm^{-1} region was assigned by second derivate.

2.5. Differential scanning calorimetry (DSC)

The glass transition temperature (T_g) of EuRL/plasticizer blends was evaluated by DSC (DSC1 Instrument, Mettler-Toledo, CH) according to the method previously described (Gennari et al., 2017).

2.6. Probe tack test

Probe tack experiments were performed on a custom-designed probe apparatus adapted on a MTS 810 hydraulic testing machine, allowing the simultaneous observation of the debonding process through a transparent glass substrate (Lakrout et al., 1999).

2.6.1. Sample preparation

In order to get films of thickness 180–200 μm on a glass slide 2.6 × 10 × 0.2 cm^3 previously cleaned and activated by a plasma technique, 2–3 mL (depending on their concentration) of each placebo formulation were deposited on each glass slide (using a perfectly levelled support plate). Each sample was dried slowly in air for 48 h and then for 30 min in an oven at 45 °C. The PSA thickness was measured by a white light scattering technique with an optical profilometer (Microsurf 3D, Fogale nanotech, Nimes, France). The resulting PSAs were stored in a container to prevent dust for the 7 days required for the matrices maturation at room temperature.

2.6.2. Experimental setup

The experiments were carried out as follows: a flat-ended probe was brought into contact with the adhesive layer at a constant probe velocity of 30 μm/s until a set compression force was reached, kept at a fixed position for a given time of 10 s, and subsequently removed at a constant crosshead speed which was varied between 1 and 1000 μm/s. Experiments were conducted at room (storage) temperature

(25 ± 0.5 °C) and at skin surface temperature (32 ± 0.5 °C). The probe was made of stainless steel with a diameter of 9.7 mm; this substrate was preferred because it is a common material with a simple behavior. Since surface roughness can affect probe test results, the degree of surface roughness was well controlled: the flat end of the probe was polished with several grades of abrasive paper; the same probe was used throughout a series of tests and its flat end was cleaned with acetone. The applied contact forces were 10, 40 and 70 N for the formulations containing 60, 50 and 40% w/w of plasticizer, respectively. During each experiment, the force, the displacement of the crosshead and the time were acquired simultaneously. Since the results are influenced by the film thickness, the force-distance curve was converted into a stress-strain curve.

The tensile stress (σ) was calculated by dividing the force registered during the detachment (F) for the contact area (A), evaluated by the video streaming, as follows:

$$\sigma = F/A \quad (1)$$

Defining h as being the time-dependent thickness of the adhesive layer and h_0 as the initial adhesive layer thickness the nominal strain (ε) was calculated as follows:

$$\varepsilon = (h - h_0)/h_0 \quad (2)$$

The area under the curve recorded by the instrument software was defined as the work of separation (W).

Selected images from recorded films were digitized and analyzed. Tests were carried out on the selected placebo formulations because the low amount of drug did not affect the adhesive and debonding mechanisms of PSAs. Each formulation was analyzed in triplicate to verify the reproducibility of the experimental conditions. A deepener description of the mechanisms which can occur during the debonding process is provided in Appendix B.

2.7. Preparation of transdermal patches

Patches were prepared by casting, using a laboratory-coating unit Mathis LTE-S(M) (Mathis, Oberhasli, CH), equipped with a blade coater. The mixture was spread on the backing layer. The coating thickness was set at 350 µm in order to obtain a dry film of about 50–100 µm. The spread mixture was dried at 60 °C for 30 min, and covered with the release liner. Finally, patches were sealed in an airtight container and stored at 25 ± 0.1 °C over a 7-day period.

2.8. Thickness of the matrices of the transdermal patches

A sample of 2.5 cm × 2.5 cm of the patch was placed between the jaws of the MI 1000 µm (ChemInstruments, Fairfield, USA). First, the whole thickness (T_W) was measured; then, the respective thicknesses of both backing layer and release liner ($T_{BL + RL}$) were measured.

The thickness of the matrix layer was calculated as $T_W - T_{BL + RL}$. The results are expressed as the mean of five measurements.

2.9. Shear adhesion

The shear adhesion was performed using an 8 Bank Oven Shear HT8 Instrument (ChemInstruments, Ichemico, Cuggiono, Italy).

2.9.1. Sample preparation

Each patch sample was cut in order to obtain specimens of 25 mm × 60 mm using three samples from each formulation. Each specimen was placed on the test panel center; it was applied to cover an area of 25 mm × 25 mm without added pressure. A clamp was placed on the masked free end of the specimen and was aligned in order to ensure a uniform distribution of the load.

2.9.2. Experimental setup

The test assembly was placed in the test stand so at an angle of 2° from vertical, minimizing the peel forces that eventually acted on the patch. A mass of 500 g was applied to the clamp (Cilurzo et al., 2015). The entire setup was enclosed in a controlled-temperature chamber in order to maintain the specimens at 32 ± 0.5 °C. The time required to completely detach the specimen from the test panel was recorded.

The results are expressed as the mean ± standard deviation of three specimens for each formulation.

2.10. Peel adhesion 180° test

The peel adhesion test at 180° measures the patch adherence when peeled at a 180° angle from a standard steel or Teflon panel (Cilurzo et al., 2005). The tests were performed using a tensile machine equipped with a 50 N cell (Instron 5965, ITW Test and Measurement Italia S.r.l., Trezzano sul Naviglio, Italy).

2.10.1. Sample preparation

Each patch sample was cut to obtain strips of 12 mm × 120 mm, and was folded about 5 mm from its release liner and a tape leader was placed on about 3 mm of the exposed patch with the adhesive side of the tape attached to the one of patch. The remainder of the tape leader was, then, folded on itself to form a double thickness leader. Then, the release liner was removed and the specimen was placed onto the Teflon test panel. The prepared specimen was first smoothed with a 2.04 kg roller, and then stored in an airtight container at 25 ± 0.1 °C for 15 min.

2.10.2. Experimental setup

The specimen was placed into the instrument with the free end of the tape leader being placed into the instrument clamp (Cilurzo et al., 2015). Six specimens were pulled from the plate at a 180° angle at a peel speed of 300 mm/min.

The average force was calculated as the arithmetic mean of all values of the linear portion of the curve. The peel values are expressed in centinewton per centimeter (cN/cm) by dividing the registered force by the width of the patch. The results are expressed as the mean ± standard deviation of six specimens for each formulation.

2.11. Cold flow

The cold flow was evaluated after a storage period of one month at 40 ± 1°C. The dimensional changes in punched-out sample were measured using a graph paper.

The evaluation was performed on samples punched in order to obtain a patch of 32 mm diameter covered with a release liner of 40 mm diameter. The samples, sealed in single airtight pocket, were stored at 40 ± 1 °C for one month. The extent of cold flow was expressed as the maximum migration of the adhesive in mm on the release liner (Fig. 1).

The cold flow was considered negligible if the PSA was not visually detectable outside the backing layer. The analysis was performed in triplicate.

2.12. Drug content

An exactly weighted 2.54 cm^2 patch sample was dissolved in 20 mL methanol by sonication (UP200st, Hielscher, Teltow, Germany) and mechanically stirred. Afterwards, the samples were left at rest for 3 h and diluted with 20 mL mobile phase described below. Each value represents the average of three measurements.

2.13. Dissolution test

The dissolution was performed by using an apparatus SR8 PLUS dissolution test station (Hanson Research, Chatsworth, USA) according

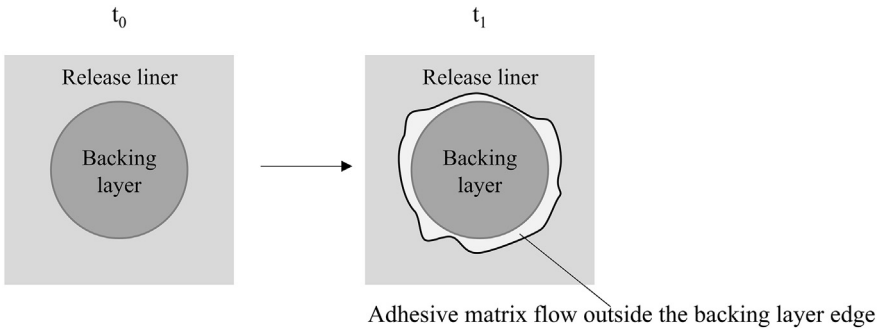

Fig. 1. Schematic representation of cold flow phenomenon.

to "Dissolution test for transdermal patches" of European Pharmacopoeia 9.1 (2017) (European Pharmacopoeia, 9th edition, 2017).

A patch sample of 8.0 cm^2 was placed flat on the disk with the release liner surface facing up. The backing layer was attached on the disk by using a cyanoacrylate adhesive. The vessels were filled with 300 mL of pH 7.4 PBS buffer, the water bath temperature was kept at 32 ± 0.5 °C, and the paddle speed was set at 25 rpm. At predetermined intervals, 5 mL samples were collected and immediately replenished with fresh medium.

The solutions were assayed by HPLC, according to the method reported below. Each result represents the average of three determinations.

The release rate constant was calculated according to the Higuchi's equation as follows:

$$M_t/M_\infty = Kt^{-0.5} \quad (3)$$

where M_t is the amount of drug released at time t, M_∞ is the drug loading in the matrix and K is the release rate constant expressed as h^{-1}.

2.14. In vitro drug permeation

2.14.1. Skin preparation

The permeation studies were performed using abdominal skin from female donors, who underwent cosmetic surgery and signed an informed consent for the use of biological samples for research purposes (Franzè et al., 2015). After removing the subcutaneous fatty tissue, skin was kept frozen until further use. For the sample preparation, adequate pieces of the frozen skin were immersed in water at 60 °C for 60 s, according to an internal protocol (Gennari et al., 2016a). After this treatment, the epidermis was carefully removed from the underlying tissue with the help of forceps. The integrity of all tissue samples was assessed measuring their electrical resistance (voltage: 100 mV, frequency: 100 Hz; Agilent 4263B LCR Meter, Microlease, Cernusco sul Naviglio, Italy), using a modified Franz diffusion cell (PermeGear, Hellertown, USA) with an effective penetration area and a receptor volume of 0.636 cm^2 and 3 mL, respectively. Samples with an electrical impedance resistance higher than 30 kΩ·cm^2 were used for the *in vitro* permeation experiments (Gennari et al., 2016b).

2.14.2. Experimental setup

The receiver compartment of Franz diffusion cell was filled with 0.9% w/v NaCl solution. Patches of 2.5 cm^2 were used as donor phase and they were applied with slight pressure with the adhesive layer in contact with the stratum corneum side before mounting the diffusion cell.

These tissue samples were sandwiched between the donor and receptor compartments of the diffusion cell, with the stratum corneum facing up the donor compartment. The upper and lower parts of the vertical Franz cell were sealed with Parafilm® and fastened together by means of a clamp. The system was kept at 37 ± 1 °C by means of a circulating water bath so that the skin surface temperature was at 32 ± 1 °C and the receiver medium was continuously maintained under stirring with a magnetic bar.

The experiments (three replicates per formulation) were performed over a 24 h period under occlusive conditions. During this period, 200 µL samples were drawn at predetermined intervals and replaced by aliquots of the receptor fluid. Sink conditions were maintained throughout the experiment. Samples were analyzed by HPLC according to the methods described below.

The cumulative amount (Q) permeated through the skin per unit of area was calculated from the concentration of each substance in the receiving medium and plotted as a function of time. The steady flux (J) was calculated as the slope of the linear portion of the plot. Finally, the efficiency of transdermal patches (E%) in drug releasing over a 24 h period was calculated as the ratio between the Q_{24h} and drug content per cent.

2.15. Drug assay

The drug concentrations in each patch, in the dissolution media and in the receiving media were quantified by HPLC analysis (Agilent HP 1100, Chemstation, Hewlett Packard, Santa Monica, USA). The following chromatographic conditions were used: *column*: HyperClone™ 5 µm BDS C18 130, 150 mm × 4.6 mm (Phenomenex, Torrance, USA); *mobile phase*: acetonitrile/water pH 2.6 (60/40, % v/v); *flow rate*: 1.5 mL/min; *wavelengths*: 225 nm (IB), 255 nm (KP) or 246 nm (FP); *temperature*: 25 °C; *injection volume*: 20 µL. The drug concentrations were determined from standard curves in the 0.1–50.0 µg/mL range.

2.16. Statistical analysis

The performances of the matrices in terms of drug release rates were compared by analysis of the variance followed by Turkey post-analyses (Daniel's XL Toolbox 6.70). The level of significance was taken as $p < 0.05$.

3. Results and discussion

3.1. Pressure sensitive adhesive physico-chemical characterization

The performances of a PSA are related to its ability to form a molecular contact with the adherent, to its rheological behavior and, obviously, to its adhesive properties. All of these characteristics are strongly dependent on the application temperature. It is generally recognized that when the glass transition temperature (T_g) of a lightly entangled and high molecular weight polymer is 25–45 °C lower than the application temperature the material becomes sticky (Zosel, 1985). Since the raw EuRL exhibited a T_g of about 63 °C and the skin temperature is about 32 °C, the addition of a plasticizer is necessary. Among the widely used plasticizers of poly(methyl methacrylate) derivatives, TBC and TRI were selected and in both the cases a minimum amount of 40% w/w of TBC and TRI was necessary to reach the target T_g value (*i.e.* $T_g < 0$ °C). Indeed, the T_g values of the EuRL plasticized

Table 1
Elastic modulus (G′) as a function of frequency and temperature, relaxation time (τ_R) and G′ at 1 Hz as function of temperature and adhesive properties (shear and peel adhesion) of placebo formulations.

Form. nos.	Solvent	EuRL	TBC	TRI	G′ (kPa)				τ_R (s)		G′ (MPa)		Shear adhesion (min)	Peel adhesion (cN/cm)
					0.05 rad/s		100 rad/s				1 Hz		32 °C	25 °C
					25 °C	32 °C	25 °C	32 °C	25 °C	32 °C	25 °C	32 °C		
1	EtOAc	60	40	–	22.98	14.19	618.47	470.61	26.31	11.11	1.86×10^{-1}	1.46×10^{-1}	1004.9 ± 9.5	14.1 ± 8.0
2	EtOAc	50	50	–	4.39	2.39	177.91	140.20	3.22	1.14	5.70×10^{-2}	4.32×10^{-2}	18.2 ± 3.5	7.5 ± 2.1
3	EtOAc	40	60	–	0.59	0.27	43.00	35.56	0.45	0.16	1.25×10^{-2}	8.59×10^{-3}	2.1 ± 0.1	3.2 ± 0.5
4	EtOAc	60	–	40	4.98	1.99	330.02	239.26	0.81	0.31	9.90×10^{-2}	6.72×10^{-2}	869.6 ± 12.4	29.1 ± 5.6
5	EtOAc	50	–	50	0.44	0.12	116.09	84.09	0.13	0.05	2.92×10^{-2}	1.83×10^{-2}	12.4 ± 2.1	17.6 ± 3.7
6	EtOAc	40	–	60	–[a]	5.97×10^{-3}	33.20	26.55	0.01	–[b]	5.57×10^{-3}	3.69×10^{-3}	0.6 ± 0.4	15.0 ± 1.7
7	iPrOH	60	40	–	3.87	1.90	279.51	192.31	0.26	0.12	7.37×10^{-2}	4.93×10^{-2}	542.1 ± 13.8	8.4 ± 2.4
8	iPrOH	60	–	40	1.61	0.58	216.84	138.53	0.18	0.08	5.75×10^{-2}	3.38×10^{-2}	393.0 ± 5.1	17.8 ± 0.7

[a] Not determined.
[b] Out of range.

with TBC and TRI at 40% w/w resulted − 20 ± 1 °C and − 7 ± 5 °C, respectively. On the basis of these data, the effect of the plasticizer on the rheological and adhesive performances of EuRL was studied in the 40–60% w/w range.

The rheological analyses revealed that, with the exception of form. no. 6, showing a distinctly liquid behavior in the considered frequency range, all the formulations were viscoelastic: at low frequency the viscous modulus (G″) was higher than the elastic modulus (G′); while at high frequency G′ dominated and a clear crossover point was visible at 25 °C (the patterns are exemplifies in Supplementary material, Fig. A1).

The influence of each variable on the rheological behavior of a PSA can be clarified by evaluating the vertical shift in elastic and viscous moduli, *i.e.* G′ and G″, and the horizontal shift of the crossover point.

In order to evaluate the structure of the PSAs in the in-use conditions, the experiments were also performed at 32 °C. As expected, even if each formulation maintained its rheological character, increasing the temperature from 25 °C to 32 °C the elastic and viscous moduli decreased (Table 1) and the relaxation time (τ_R), defined by $1/\omega$ at the crossover point between the storage (G′) and viscous (G″) moduli, decreased according to an increase of the fluidity of the system.

The increasing of the relative amount of each plasticizer (from 40 to 60% w/w) caused shifts in the elastic and viscous moduli at each frequency (Table 1).

Fig. 2a shows the rheological results obtained by analyzing the formulations containing different amounts of TBC (form. no. 1, 2 and 3) at 25 °C. Even if all these formulations are viscoelastic fluids, the PSAs become more fluid increasing the plasticizer amount. Indeed, the observed relaxation time decreased when increasing the amount of TBC (Table 1).

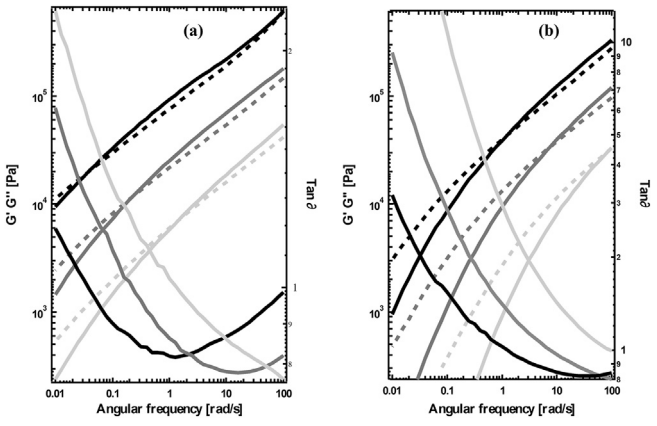

Fig. 2. Evolution of G′ (solid line) and G″ (dashed line) as a function of frequency. (a) formulations containing TBC and (b) formulations containing TRI (black line: formulations containing 40% w/w of plasticizer, grey line: formulations containing 50% w/w of plasticizer and light grey line: formulations containing 60% w/w of plasticizer). Tests were performed at 25 °C.

Moreover, TRI appeared a better plasticizer of EuRL than TBC. Indeed, it was clear by frequency sweep measurements at 25 °C that formulations containing TRI are more liquid, showing higher terminal relaxation times (Fig. 2b and Table 1). As already stated above, at the highest concentration of plasticizer, the PSA containing TRI showed a liquid behavior, while the PSA containing TBC at the same concentration behaved as a viscoelastic material.

This effect cannot be merely ascribed to the differences in miscibility of TBC or TRI with EuRL. Indeed, the solubility parameters (∂, see Appendix B for more details), calculated for these plasticizers ($\partial_{TBC} = 18.86\ MPa^{1/2}$; $\partial_{TRI} = 20.82\ MPa^{1/2}$) and for EuRL ($\partial_{EuRL} = 21.24\ MPa^{1/2}$) according to the Fedors method (Fedors, 1974), resulted almost superimposable. Thus, the different effects of the selected plasticizers on the EuRL rheological behavior can only be attributed to different specific interactions. The comparison of ATR-FTIR spectra recorded on the raw materials and different PSAs showed significant modifications in the 1800–1650 cm^{-1} region attributed to the stretching of the carbonyl moieties of the copolymer and plasticizers (the whole spectra are reported in Supplementary material Fig. A2). In this region, independently of the PSA composition, the intensity of the C═O band decreased with respect to that registered on raw materials, suggesting a possible interaction between EuRL and the two plasticizers mediated by H-bonds. This reduction of the carbonyl peak intensity was accompanied by a significant shift of the band toward higher wavenumbers (Fig. 3a and b). Shifts to higher wavenumbers associated with lower intensities of C═O stretching bands can be related to the formation of novel H-bonds which determines changes in electron densities on different atoms (Piermaria et al., 2011). Since these events are more evident in the spectra registered on PSA made of EuRL-TRI (Fig. 3b) than on those made of EuRL-TBC (Fig. 3a), it is reasonable to hypothesize that TRI interacted with EuRL more strongly than TBC, in agreement with the higher plasticizing effect verified in the rheological studies.

Focusing now on the adhesive properties, it should be considered that the initial bonding of a PSA on an irregular surface, like the skin, is driven by the wettability and flow properties at low frequencies. Moreover, Dahlquist suggested that a sufficient level of adhesion is reached when the PSA exhibits an elastic shear modulus lower than 0.1 MPa measured at 1 Hz frequency (Dahlquist, 1969). As shown in Table 1, all the formulations fulfill the so-called Dahlquist criterion of tackiness with the only exception of form. no. 1 showing a slightly higher, but still acceptable, G′ value either at room temperature and skin temperature.

The performances of the designed formulations were, then, further

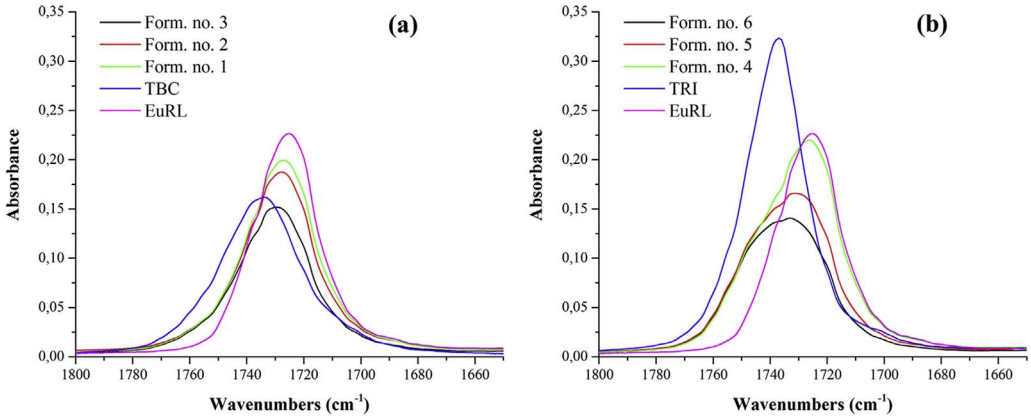

Fig. 3. ATR-FTIR spectra of C═O bands of the raw materials and formulations 1–6 in the 1650–1800 cm^{-1} region.

characterized by studying the debonding mechanism during the tack tests.

The compression force to apply during the experiment was preliminary evaluated for each sample (performing different tests at different contact forces) in order to maintain constant the indentation of the probe in the adhesive layer (maximum 15 μm); the objective was to impose a contact force that causes an indentation that did not influence the shape of the stress-strain curve.

Generally speaking, detachment patterns in probe tests are mainly governed by the extent of plasticizer in the formulation. Fig. 4a exemplifies the typical stress-strain curve observed for the formulations with the lowest plasticizer concentration. The detachment pattern shows an initial cavitation occurring at the interface between the probe and the PSA; the deformation of the layer during the debonding process was low with mainly lateral propagation and coalescence of the initial cavities along the interface and a decrease in nominal stress.

This mechanism of debonding, and, therefore, the shape of the stress-strain curves were not influenced much by changing the type of plasticizer (form. no. 7 *vs* 8) or the solvent used for the preparation of the PSA (form. no. 7 *vs* 1 and 4 *vs* 8) as shown in Fig. 5.

Increasing the debonding rate, independently of the temperature, the maximum nominal stress and the work of adhesion increased significantly (Fig. 6a and b), at least up to the values taken into consideration. This behavior can be attributed to the viscoelastic losses occurring in the adhesive layer, which increase with increasing deformation rate.

In order to evaluate the behavior of each PSA in the in-use conditions, experiments were also performed at 32 °C. No significant modifications in the adhesive and detachment properties were observed.

Increasing the amount of both the plasticizer from 40% w/w to 60% w/w, the maximum stress decreased, while the maximum nominal strain increased (Fig. 6c and d). These trends were observed for all the tested debonding velocities, in each experimental condition.

Keeping constant the EuRL/plasticizer ratio at 40/60 w/w, the two formulations showed the same detachment pattern and very similar stress-strain curves (Fig. 4b), even if they presented somewhat different rheological properties. Indeed, the debonding process was governed by a viscous flow, independently of the debonding rate and temperature. Four different stages were identified: (i) homogeneous deformation corresponding to a rapid increase of the force and no optically visible voids; (ii) nucleation and rapid growth of voids at the probe-film interface, close to the point where the nominal stress goes through a maximum; (iii) slow growth of these voids until they occupy most of the initial contact area; (iv) air penetration into the voids and breakage of the bonds with the formation of isolated fibrils that eventually break (cohesive failure).

It is interesting to note that both the formulations containing 50% w/w of plasticizer showed the first type of debonding mechanism at the higher debonding velocities (100 and 1000 μm/s); while at 10 μm/s they presented the second pattern, even if no residues were optically visible at the end of the experiments. This feature may be attributed to the fact that at lower debonding velocity the polymeric chains have

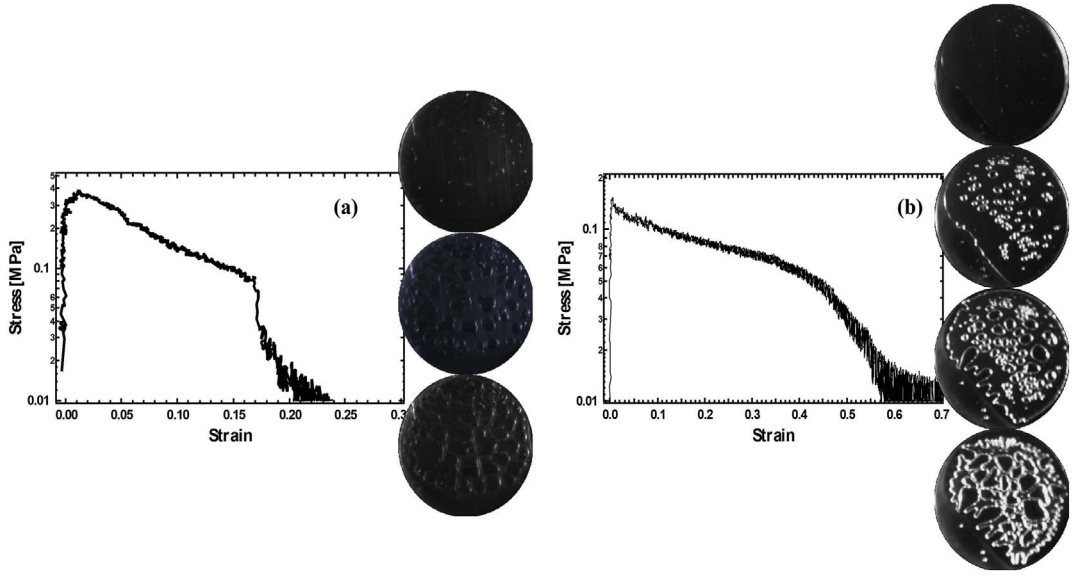

Fig. 4. Typical stress-strain curves, schematic and video captures of the debonding mechanism at 10 μm/s and 25 °C of (a) formulation no. 8 and (b) 6.

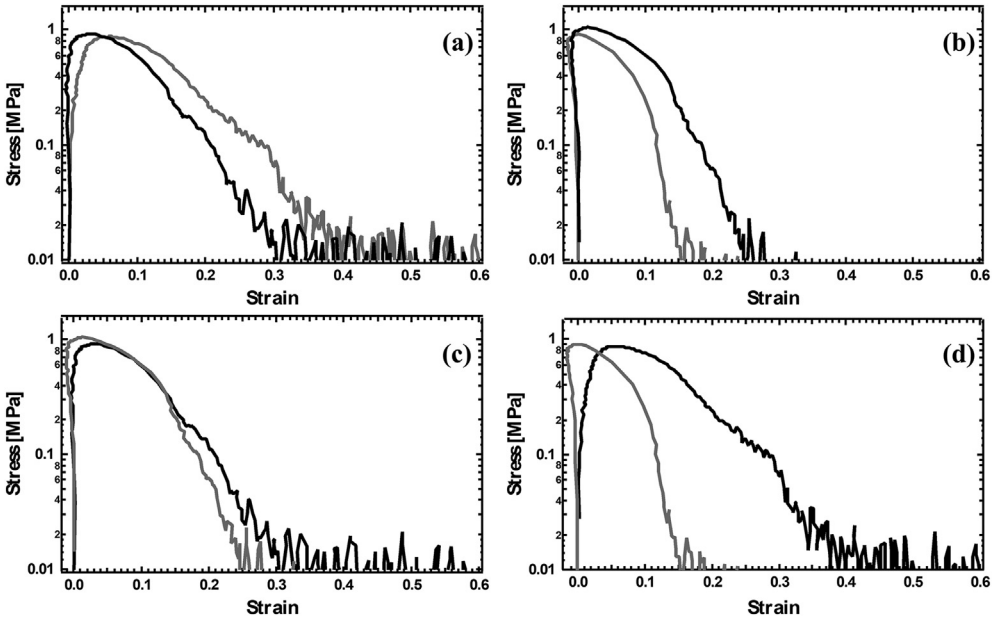

Fig. 5. Stress-strain curves of the formulations with (a) 40% w/w of plasticizer and ethyl acetate as solvent (black line: TBC, grey line: TRI); (b) 40% w/w of plasticizer and isopropanol as solvent (black line: TBC, grey line: TRI); (c) 40% w/w of TBC (black line: ethyl acetate, grey line: isopropanol) and (d) 40% w/w of TRI (black line: ethyl acetate, grey line: isopropanol). Tests were performed at 100 μm/s and 32 °C. Note that negative slopes in the loading part of the curve are due to an overcorrection of the compliance of the machine, but do not affect the measured adhesion energy (integral under the curve).

time to re-organize and the PSA has time to relax.

3.2. Characterization of placebo patches

The results on the shear adhesion are shown in Table 1. They represent the resistance of the matrix to flow (Minghetti et al., 2004). The shear adhesion test measures the ability of a patch to adhere to a standard steel panel under a constant shear stress. Since the detachment of the patch from the stainless steel surface occurred cohesively, the data obtained by shear adhesion test can be considered as a true measure of the cohesive strength of the PSA. The increase in plasticizer content caused a reduction in shear adhesion values, due to the dilution of the entanglements of the polymer, resulting in a flowing matrix. This effect appeared clearly with both the plasticizers, in agreement with the pattern found in the rheological measurements at 0.05 rad/s (Table 1). However, excluding form. no. 6, all shear adhesion values could be considered suitable for the development of a patch intended for drug administration (Cilurzo et al., 2010).

The comparison of the shear adhesion values also revealed that the solvent used to prepare the formulation had an impact on the creep resistance of placebo formulations, since the patches prepared in isopropanol showed lower shear adhesion values (form. nos. 7 and 8, Table 1) relative to those prepared in ethyl acetate, in agreement with the rheological studies.

Shifting from shear adhesion to peel adhesion, that represents the force required to peel away a patch from a substrate, it is noteworthy that only the patches prepared with the highest amount of plasticizer left residues on the stainless steel panel, confirming the low cohesive properties of the formulation. Consequently, in order to compare all the formulations, the experiments were repeated using a Teflon® panel which presents a lower critical surface tension (Kim et al., 2005). In presence of TRI, the peel adhesion values appeared slightly higher than

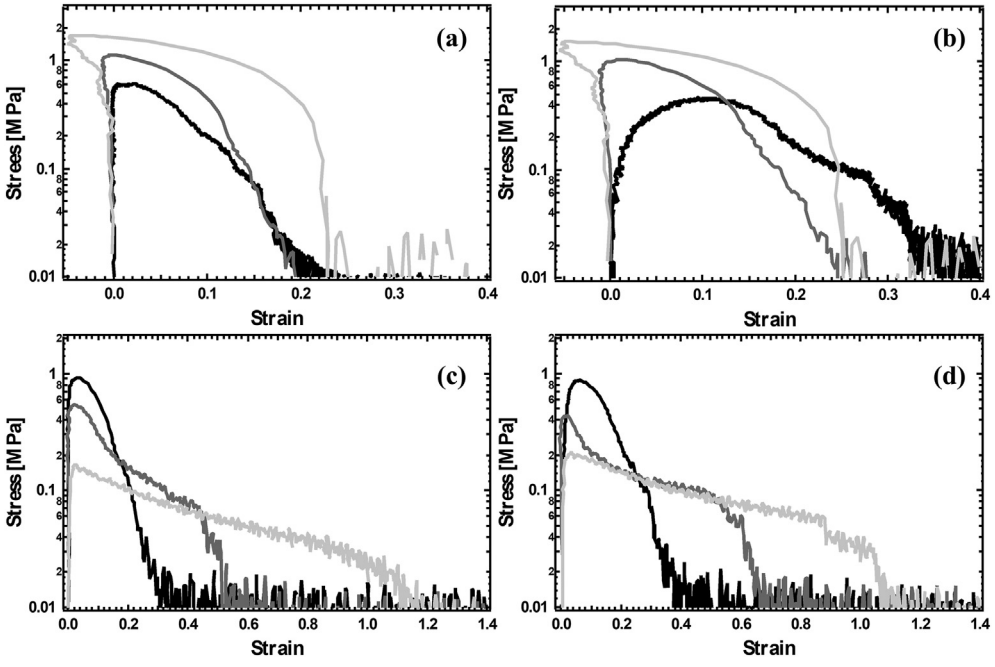

Fig. 6. Effect of the debonding velocity (a and b) and of the plasticizer amount (c and d) on the stress-strain curves. Formulation no. 7 tested at (a) 25 °C and (b) 32 °C (light grey line: 1000 μm/s, grey line: 100 μm/s, black line: 10 μm/s). Formulations containing (c) TBC and (d) TRI (black line: formulations with 40% w/w of plasticizer, grey line: formulations with 50% w/w of plasticizer, light grey line: formulations with 60% w/w of plasticizer).

those of the corresponding patches prepared with TBC (Table 1). In both cases, the peel adhesion values decreased with increasing the plasticizer concentration. However, the relatively low peel force values obtained can be considered satisfactory, since higher values could cause pain or skin damage upon the patch removal.

Cold flow, a phenomenon similar to drug leakage from the edge of membrane-controlled patch, is one of the possible product quality defects (Wokovich et al., 2006). It represents the migration of the PSA outside the edge of the backing layer during the storage and it occurs when the matrix flows like a very viscous liquid between the backing layer and the release liner during the storage. As an example, this negative effect may result in a patch stuck to the primary packaging container becoming unusable. Both the formulations containing 60% w/w of plasticizer presented cold flow after one month of storage at 40 °C, in agreement with the rheological data and independently of the type of plasticizer; while this phenomenon was absent when 40–50% w/w of plasticizers was used. These results on placebo patches are consistent with the data reported by Lin et al. (2000) who reported that the minimum amount of TRI and TBC required to obtain a positive answer to the rolling ball tack test was about 35% and 40%, respectively. Similarly, 40% of di-butyl-phthalate was required. Indeed, when this plasticizer was used at lower concentrations (*i.e.* 30% and 20%) to develop transdermal patches containing risperidone (Aggarwal et al., 2013) and verapamil (Kusum et al., 2002), it would not be enough to conferee suitable adhesive properties to the patch. Indeed, since the patch was fixed to animal skin, probably, the rheological and adhesive properties were not sufficient to guarantee the residence of the patch on application site over the required time period.

3.3. Characterization of the drug-loaded patches

Since the drugs loaded polymeric mixtures prepared by using ethyl acetate shrunk after casting on the release liner, the drug loaded patches were prepared using only isopropanol as solvent. In all cases, the drug content complied the Ph. Eur assay for the uniformity of dosage units (Table 3).

The loading of the selected active ingredients, namely IB, KP and FP, to the matrices containing TRI did not significantly influenced the debonding patterns (data not shown), peel adhesion and shear adhesion values (Tables 2 and 3). These data were in agreement with the lack of modification on the rheological pattern suggesting that the loaded drug did not modify the interactions occurring between EuRL and TRI. Conversely, in the case of the adhesive matrices prepared using TBC, a reduction of about 20% shear adhesion values was found (Tables 2 and 3) probably because of a plasticizing effect exerted by the loaded drugs (Tables 2 and 3). It can be assumed that the drug can disrupt the interactions occurring between TBC and EuRL in favor of the formation of H-bonds between the carboxylate of the drug and the ester moieties of the copolymer (Cilurzo et al., 2005; Pignatello et al., 2001). The lack of significant differences due to the loaded drug can be justified on the bases of the solubility parameters. Indeed, all the three compounds can be considered freely mixable with EuRL being their values (IB: 20.91 $MPa^{1/2}$; KP: 23.23 $MPa^{1/2}$; FP: 21.53 $MPa^{1/2}$) close to that of the placebo adhesive matrix (EuRL/TBC 60/40: 20.28 $MPa^{1/2}$).

Since the therapeutic performances of a transdermal patch are affected not only by its adhesive properties, which assure the residence time of the drug on the skin surface, but also by the ability of the patch itself to release the drug, both the *in vitro* drug release and *in vitro* drug skin permeation were determined.

Table 3 shows the drug release constants calculated according to the Higuchi model.

These data were in agreement with the rheological results on the effect of the type of plasticizer. The patches containing TRI presented significantly higher release constants ($p < 0.05$) due to the more pronounced plasticizing effect: the lower the G′ values at each frequency and, more important, the shorter the relaxation time, the higher the viscous characteristic of the PSA at a given temperature and the faster the release rate (Tables 2 and 3). Hence, the presence of TRI increased the mobility of the polymeric chains favoring the diffusion of the drug through the matrix.

The *in vitro* drug release can be considered satisfactory for all formulations since it was almost complete within 7 h independently of the plasticizer type (see Supplementary material Fig. A3). Thus, the plasticizer was selected only on the bases of the adhesive properties and, therefore, the *in vitro* skin permeation studies were carried out on formulations containing TBC (the skin permeation profiles are reported in Supplementary material, Fig. A3b).

PSA made of EuRL and TBC in the 60/40 w/w ratio allowed to obtain a prolonged permeation profile of the loaded drug over least 24 h. Moreover, it should be underlined that the efficiency of transdermal patches in drug releasing over a 24 h period (E%, Table 3) resulted almost double with respect to commercially available plasters containing flurbiprofen (Transact®, Cilurzo et al., 2015) and ibuprofen (Ibupas®, Cilurzo et al., 2015) and slightly lower with respect that loaded with ketoprofen (Keplat®, Cilurzo et al., 2015).

The increased mobility (or lower viscosity) caused by the selected drugs did not have a significant influence on the permeation process. Indeed, the τ_R values taken as representative of the rheological pattern, did not match with the drug fluxes through the skin, suggesting that the barrier properties of the stratum corneum ruled the skin permeation process. In other words, drug permeation pattern after the application of a patch on the skin is governed by different mechanisms (Kalia and Guy, 2001) with respect to the *in vitro* drug release. In particular, the flux determined for KP was about 5-fold lower than FP and IB, which were not statistically different ($p > 0.05$). The same trend was found by Swart et al. (2005) using aqueous saturated solution as the reported KP flux was about 4 fold lower than those measured in the case of FP and IB, which were not significantly different. Hence, the overall data suggested that the skin permeation process was not influenced by the formulation in a PSA made of EuRL and TBC, but only by the physicochemical characteristics of the loaded drug which dictates the diffusion process through the stratum corneum.

Table 2
Elastic modulus (G′) as a function of frequency and temperature, relaxation time (τ_R) as a function of temperature and adhesive properties (shear and peel adhesion) of drug-loaded formulations.

Form. nos.	Solvent	EuRL	TBC	TRI	Drug	G′ (kPa)				τ_R (s)		Shear adhesion (min)	Peel adhesion (cN/cm)
						0.05 rad/s		100 rad/s					
						25 °C	32 °C	25 °C	32 °C	25 °C	32 °C	32 °C	25 °C
9	iPrOH	60	40	–	IB	2.85	1.37	244.96	182.75	0.25	0.10	433.0 ± 5.3	8.9 ± 0.2
10	iPrOH	60	40	–	KP	1.03	0.53	157.85	128.21	0.20	0.07	420.8 ± 1.6	5.2 ± 2.5
11	iPrOH	60	40	–	FP	1.97	0.79	215.90	134.22	0.23	0.08	430.1 ± 0.6	8.8 ± 3.1
12	iPrOH	60	–	40	IB	1.16	0.49	157.85	117.64	0.17	0.07	385.7 ± 5.4	12.2 ± 0.8
13	iPrOH	60	–	40	KP	0.90	0.33	160.91	117.86	0.13	0.05	388.2 ± 1.0	36.4 ± 2.1
14	iPrOH	60	–	40	FP	1.34	0.53	188.61	142.71	0.16	0.07	380.6 ± 2.1	9.8 ± 0.4

Table 3
Drug content, drug release constants and main parameters calculated from *in vitro* skin permeation experiments (drug flux, *i.e. J*; cumulative drug amount permeated, *i.e.* Q_{24h}; efficiency of transdermal patches, E%) of drug-loaded patches.

Form. nos.	Solvent	EuRL	TBC	TRI	Drug	Drug content (μg/cm^2)	K (h^{-1})	*J* (μg/cm^2/h)	Q_{24h} (μg/cm^2)	E% (%)
9	iPrOH	60	40	–	IB	153.0 ± 4.2	0.58 ± 0.04	2.35 ± 0.41	51.26 ± 7.42	33.5 ± 4.8
10	iPrOH	60	40	–	KP	159.9 ± 3.8	0.57 ± 0.01	0.45 ± 0.22	24.14 ± 4.10	15.1 ± 2.6
11	iPrOH	60	40	–	FP	120.4 ± 5.1	0.38 ± 0.03	1.63 ± 0.17	29.57 ± 11.32	24.6 ± 9.4
12	iPrOH	60	–	40	IB	131.3 ± 4.3	0.67 ± 0.01	-*	-*	-*
13	iPrOH	60	–	40	KP	171.5 ± 10.9	0.78 ± 0.01	-*	-*	-*
14	iPrOH	60	–	40	FP	130.8 ± 14.7	0.51 ± 0.07	-*	-*	-*

-*: not determined.

4. Conclusion

The current work allowed defining the rheological and adhesive properties of highly plasticized EuRL. The results permitted to identify the optimal copolymer/plasticizer ratio and evidenced the relevance of the PSA rheological behavior on the adhesive properties, reflecting on debonding pattern and shear adhesion. In the specific case of EuRL, the optimal polymer/plasticizer ratio was in the 60/40–50/50% w/w range for both TBC and TRI. The selected drugs loaded at 4% w/w decreased the relaxation time, as an indication of the increase of the matrix fluidity. This behavior has a beneficial impact on the *in vitro* release, determined by dissolution test: the shorter the relaxation time, the higher the drug release rate.

In conclusion, the knowledge of viscoelastic properties of the PSA appears crucial to identify the formulation space during the development of transdermal patches and/or medicated plasters and to optimize their performances. In particular, the matrix relaxation time appears a suitable parameter to optimize the copolymer/plasticizer ratio and establish the possible influence of the active ingredient.

Supplementary data to this article can be found online at https://doi.org/10.1016/j.ejps.2017.10.006.

References

Aggarwal, G., Dhawan, S., Harikumar, S., 2013. Formulation, in vitro and in vivo evaluation of transdermal patches containing risperidone. Drug Dev. Ind. Pharm. 39 (1), 39–50.

Cilurzo, F., Minghetti, P., Casiraghi, A., Tosi, L., Pagani, S., Montanari, L., 2005. Polymehacrylates as crystallization inhibitors in monolayer transdermal patches containing ibuprofen. Eur. J. Pharm. Biopharm. 60, 61–66.

Cilurzo, F., Minghetti, P., Gennari, C.G.M., Casiraghi, A., Montanari, L., 2010. A novel polymethylmethacrylate hydrophilic adhesive matrix intended for transdermal patch formulations. Drug Deliv. 17 (3), 171–177.

Cilurzo, F., Gennari, C.G.M., Minghetti, P., 2012. Adhesive properties: a critical issue in transdermal patch development. Expert Opin. Drug Deliv. 9 (1), 33–45.

Cilurzo, F., Selmin, F., Gennari, C.G.M., Montanari, L., Minghetti, P., 2014. Application of methyl methacrylate copolymers to the development of transdermal or loco-regional drug delivery systems. Expert Opin. Drug Deliv. 11 (7), 1022–1045.

Cilurzo, F., Gennari, C.G.M., Selmin, F., Franzé, S., Musazzi, U.M., Minghetti, P., 2015. On the characterization of medicated plasters containing NSAIDs according to novel indications of USP and EMA: adhesive property and in vitro skin permeation studies. Drug Dev. Ind. Pharm. 41 (2), 183–189.

Creton, C., Leibler, L., 1996. How does tack depend on time of contact and contact pressure? J. Polym. Sci. B Polym. Phys. 34 (3), 545–554.

Dahlquist, C.A., 1969. Pressure-sensitive adhesives. In: Patrick, R.L. (Ed.), Treatise on Adhesion and Adhesives. Marcel Dekker Inc., New York, pp. 219–260.

Deplace, F., Carelli, C., Mariot, S., Retsos, H., Chateauminois, A., Ouzineb, K., Creton, C., 2009. Fine tuning the adhesive properties of a soft nanostructured adhesive with rheological measurements. J. Adhes. 85 (1), 18–54.

European Pharmacopoeia, 9th edition, 2017. Dissolution Test for Transdermal Patches 01/2008: 20904. pp. 309–310.

Fauth, C., Wiedersberg, S., Neubert, R.H., Dittgen, M., 2002. Adhesive backing foil interactions affecting the elasticity, adhesion strength of laminates, and how to interpret these properties of branded transdermal patches. Drug Dev. Ind. Pharm. 28 (10), 1251–1259.

Fedors, F.F., 1974. A method for estimating both the solubility parameters and molar volumes of liquids. Polym. Eng. Sci. 14 (2), 147–153.

Franzè, S., Gennari, C.G.M., Minghetti, P., Cilurzo, F., 2015. Influence of chemical and structural features of low molecular weight heparins (LMWHs) on skin penetration. Int. J. Pharm. 481, 79–83.

Gennari, C.G.M., Franzé, S., Pellegrino, S., Corsini, E., Vistoli, G., Montanari, L., Minghetti, P., Cilurzo, F., 2016a. Skin penetrating peptide as a tool to enhance the permeation of heparin through human epidermis. Biomacromolecules 17 (1), 46–55.

Gennari, C.G.M., Selmin, F., Ortenzi, M.A., Franzé, S., Musazzi, U.M., Casiraghi, A., Minghetti, P., Cilurzo, F., 2016b. In situ film forming fibroin gel intended for cutaneous administration. Int. J. Pharm. 511 (1), 296–302.

Gennari, C.G.M., Selmin, F., Franzè, S., Musazzi, U.M., Quaroni, G.M.G., Casiraghi, A., Cilurzo, F., 2017. A glimpse in critical attributes to design cutaneous film forming systems based on ammonium methacrylate. J. Drug Delivery Sci. Technol. 41, 157–163.

Kalia, Y.N., Guy, R.H., 2001. Modeling transdermal drug release. Adv. Drug Deliv. Rev. 48 (2–3), 159–172.

Kim, D.J., Kim, H.J., Yoon, G.H., 2005. Effect of substrate on peel strength of SIS(styrene-isoprene-styrene)-based HMPSAs. Int. J. Adhes. Adhes. 25 (4), 288–295.

Kusum, D.V., Saisivam, S., Maria, G.R., Deepti, P.U., 2002. Design and evaluation of matrix diffusion controlled transdermal patches of verapamil hydrochloride. Drug Dev. Ind. Pharm. 29 (5), 495–503.

Lakrout, H., Sergot, P., Creton, C., 1999. Direct observation of cavitation and fibrillation in a probe tack experiment on model acrylic pressure-sensitive-adhesives. J. Adhes. 69 (3–4), 307–359.

Lin, S., Chen, K., Run-Chu, L., 2000. Organic esters of plasticizers affecting the water absorption, adhesive property, glass transition temperature and plasticizer permanence of Eudragit acrylic films. J. Control. Release 68 (3), 343–350.

Minghetti, P., Cilurzo, F., Casiraghi, A., 2004. Measuring adhesive performance in transdermal delivery systems. Am. J. Drug Deliv. 2 (3), 193–206.

Nase, J., Lindner, A., Creton, C., 2008. Pattern formation during deformation of a confined viscoelastic layer: from a viscous liquid to a soft elastic solid. Phys. Rev. Lett. 101 (7), 074503.

Piermaria, J., Bosch, A., Pinotti, A., Yantorno, O., Garcia, M.A., Abraham, A.G., 2011. Kefiran films plasticized with sugars and polyols: water vapor barrier and mechanical properties in relation to their microstructure analysed by ATR/FT-IR spectroscopy. Food Hydrocoll. 25, 1261–1269.

Pignatello, R., Ferro, M., Puglisi, G., 2001. Preparation of solid dispersions of nonsteroidal anti-inflammatory drugs with acrylic polymers and studies on mechanisms of drug-polymer interactions. AAPS PharmSciTech 3 (2), E10.

Swart, H., Breytenbach, J.C., Hadgraft, J., du Plessis, J., 2005. Synthesis and transdermal penetration of NSAID glycoside esters. Int. J. Pharm. 301 (1–2), 71–79.

Tan, H.S., Pfister, W.R., 1999. Pressure-sensitive adhesives for transdermal drug delivery systems. Pharm. Sci. Technol. Today 2 (2), 60–69.

The European Agency for the Evaluation of Medicinal Products. Guideline on quality of transdermal patches, London, 23 October 2014, EMA/CHMP/QWP/608924/2014.

Wokovich, A.M., Prodduturi, S., Doub, W.H., Hussain, A.S., Buhse, L.F., 2006. Transdermal drug delivery system (TDDS) adhesion as a critical safety, efficacy and quality attribute. Eur. J. Pharm. Biopharm. 64 (1), 1–8.

Zosel, A., 1985. Adhesion and tack of polymers: influence of mechanical properties and surface tensions. Colloid Polym. Sci. 263 (7), 541–553.